SCHWEIZ. MINERAL. PETROGR. MITT. 74, 343–358, 1994

Rb–Sr systematics of recrystallized shear zones at the greenschist-amphibolite transition: examples from granites in the Swiss Central Alps

by *D. Marquer*[1] and *J.J. Peucat*[2]

Abstract

In the Swiss Central Alps, several metagranite ductile shear zones which have undergone various metamorphic conditions (350 to 600 °C and 3 to 7 kb) were analysed for their Rb–Sr systematics. In the greenschist facies, the rubidium content increases in mylonites while the strontium content decreases. Opposite chemical variations are observed in amphibolite facies shear zones. These chemical mass transfers reflect the different behaviour of the initial magmatic paragenesis during deformation. In amphibolite facies, the initial paragenesis is stable, K-feldspar and oligoclase recrystallize to a fine grained mylonite. In the greenschist facies, the feldspathic phase is progressively replaced by a new metamorphic assemblage (quartz-phengite-albite). In both metamorphic cases, Sr isotope changes of the whole rocks are strongly suspected to occur in the mylonites. These chemical and isotopic modifications are probably related to external fluid circulation and are also affected by progressive mineral changes.

In each studied area, the whole rock Rb–Sr isotopic dating method records magmatic ages of the undeformed granite, while spurious ages with respect to tectonic events are obtained for mylonites in shear zones.

Keywords: granite, shear zone, mylonite, Rb–Sr systematics, Central Alps, Switzerland.

Introduction

During heterogeneous deformation, granitoids may undergo different changes in major and minor element contents and stable isotope ratios in shear zones dependent of the physical parameters (mainly temperature), the mineralogical modifications (mainly controlled by the feldspar phases) and the presence of fluids (see review in MARQUER, 1989; DIPPLE et al., 1990; TOBISCH et al., 1991; SELVERSTONE et al., 1991). Over the past several decades, geologists have focused their interest on the understanding of some theoretical aspects of fluid-rock interaction, fluid circulation, fluid sources and the role of fluids for the rheology of rocks (FYFE et al., 1978; FERRY, 1979; ETHERIDGE et al., 1983, BICKLE and MCKENZIE, 1987; RUMBLE, 1989; MCCAIG et al., 1990; FERRY and DIPPLE, 1991). These studies of chemical mass-transfer indicate changes in major and minor element concentrations and strong modifications of stable isotope ratios in many shear zones (KERRICH et al., 1980, 1984; MCCAIG, 1984, 1989; ETHERIDGE et al., 1984; WINSOR, 1984; BRODIE and RUTTER, 1985; MARQUER et al., 1985; SINHA et al., 1986; FOURCADE et al., 1989; DIPPLE et al., 1990; TOBISCH et al., 1991; SELVERSTONE et al., 1991; and see review in MARQUER, 1989).

Up to now, however, little is known about the modifications of Rb–Sr isotope systematics in mylonitized granites (ABBOTT, 1972; ETHERIDGE and COPPER, 1981; THÖNI, 1983, 1986; MAJOOR, 1988; BAROVICH and PATCHETT, 1992). From a general point of view, plutonic rocks deformed syn- and post-intrusively must be distinguished. In the first case, whole rock ages in mylonites appear to correspond to tectono-magmatic events when only changes in the Rb/Sr ratio occur (BOSSIÈRE, 1980; PEUCAT, 1983). In the second case, relations between deformation processes and apparent isotopic ages seem to be much more complex. Some authors assert that

[1] Institut de géologie, E. Argand, 11, CH-2007 Neuchâtel, Switzerland.
[2] Géosciences, Laboratoire de géochimie-géochronologie Campus de Beaulieu, F-35042 Rennes, France.

isotopic rehomogenization occurs during deformation, therefore the determined ages should correspond to the mylonitization event (HARPER and LANDIS, 1967; DIETRICH et al., 1969; HUNZIKER, 1970; ABBOT, 1972; STEINITZ and JÄGER, 1981; HICKMANN, 1984; STEINER, 1984). On the other hand, ETHERIDGE and COOPER (1981) argued for mobility of rubidium and strontium on a large scale, enhanced by fluid circulation. In this case, the whole rock isochron gives no indication of the age of the retrograde event. With these conflicting results, the discussion about the significance of whole rock Rb–Sr dating of deformed granites is still open and is of a great importance because the Rb–Sr system is often used to date tectono-metamorphic events responsible for mountain building (for review see, HURFORD et al., 1989).

The present study describes the effects of Alpine mylonitization on Rb–Sr whole-rock systems of late Variscan granites in the Swiss Central Alps (Fig. 1). The studied metagranites underwent heterogeneous ductile deformation under different metamorphic conditions. In the case of the Wassen granite, Aar granite and the Grimsel granodiorite, this occurred under greenschist facies and in the case of the Truzzo granite under amphibolite facies (FREY et al., 1974, 1980) (Fig. 2). The purpose of this paper is to document and compare the behaviour of the Rb–Sr whole rock system in structurally and chemically well-defined metagranite shear zones (MARQUER et al., 1985, FOURCADE et al., 1989; MARQUER, 1989, 1991). In particular, this study focuses on the relationships between deformation, chemical mass transfer and whole rock dating at the transition from greenschist to amphibolite facies. This paper presents in detail the following points: the validity and significance of intrusion ages defined in the metagranites, the relationships between mass transfer, deformation and metamorphic conditions and the effects of these chemical modifications on the Rb–Sr isotope diagrams.

Geological setting and timing of Alpine deformation

The Aar and Gotthard massifs, the so-called External Crystalline Massifs (ECM), are located in the northern part of the Swiss Central Alps (Fig. 1). The ECM are mainly composed of old crystalline rocks and late Variscan granites (STECK, 1966; LABHART, 1977; SCHALTEGGER, 1990a; ABRECHT, 1994; MERCOLLI et al., 1994; SCHALTEGGER, 1994). In these Variscan granites, Alpine heterogeneous deformation led to the formation of ductile shear zones surrounding lenses of weakly deformed rocks (CHOUKROUNE and GAPAIS, 1983; GAPAIS et al., 1987). At all scales, the geometry of this heterogeneous deformation shows anastomosing patterns of shear zones corresponding to a bulk vertical stretching (MARQUER and GAPAIS, 1985). On the basis of the evolution of thrust tectonics and deformation of the foreland flysch and molasse sequences (TRÜMPY, 1980; BREITSCHMID, 1982; PFIFFNER, 1986) and cooling ages of syntectonic minerals in deformed samples (STEIGER, 1964; JÄGER et al., 1967; DEUTSCH and STEIGER, 1985; DEMPSTER, 1986), the main ductile deformation of the ECM can be attributed to late Oligocene time. The analyzed metagranite shear zones, which have undergone greenschist facies conditions, are located in the Aar massif (Fig. 1), in the Hasli valley for the Aar granite and Grimsel granodiorite (between Handegg and the Grimsel pass) and in the Reuss valley for the Wassen granite (near the village of Wassen).

The shear zones that developed under amphibolite facies conditions have been sampled in the Truzzo granite near the Liro valley and the Truzzo lake, north of Chiavenna (Italy). The Truzzo granite belongs to the Penninic domain (TRÜMPY, 1980). Geologically, this granite is a part of the Tambo nappe, located between the Adula and the Suretta nappes (Fig. 1). Ductile Alpine deformation is heterogeneous, leading to the development of a complex pattern of shear zones surrounding lenses of weakly deformed granitic rocks (WEBER, 1966; MARQUER, 1991). Four distinct deformation events have been recognized in

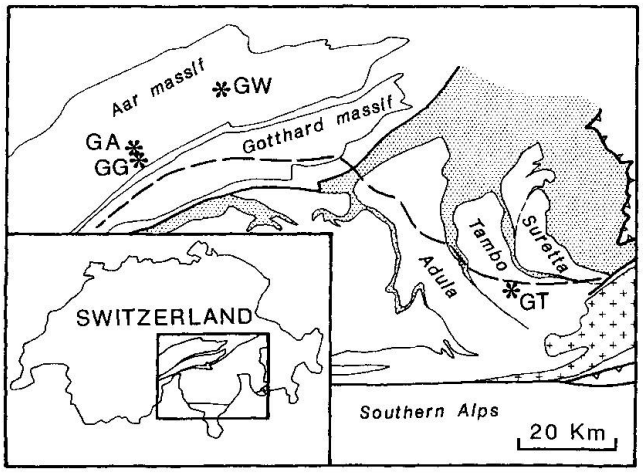

Fig. 1 Location of the metagranite shear zones. GT: Truzzo granite (Tambo nappe); GG: Grimsel granodiorite (Aar massif); GA: Aar Granite (Aar massif); GW: Wassen granite (Aar massif). The dashed line corresponds to the greenschist facies – amphibolite facies boundary.

the Truzzo granite (MARQUER, 1991). On the basis of the principal directions of finite strain, metamorphic paragenesis and observation of superposed structures, it is possible to relate the various shear zones to different deformation events. High temperature shear zones were developed during the main deformation (D2) event and correspond to pronounced E–W stretching and vertical shortening (MARQUER, 1991). Based on structural studies of the thrusting of the Penninic basement units over Eocene flysch sediments (SCHMID et al., 1990) and on isotopic dating (JÄGER et al., 1967; STEINITZ and JÄGER, 1981; DEUTSCH and STEIGER, 1985), the Lepontine metamorphism and deformation (D2) in this area is estimated to have occurred during the early Oligocene (HURFORD et al., 1989; MARQUER et al., 1994). Only results from metagranite shear zones generated during deformation D2 are presented here because these deformation zones have not undergone strong ductile reactivation during late stages of Alpine deformations.

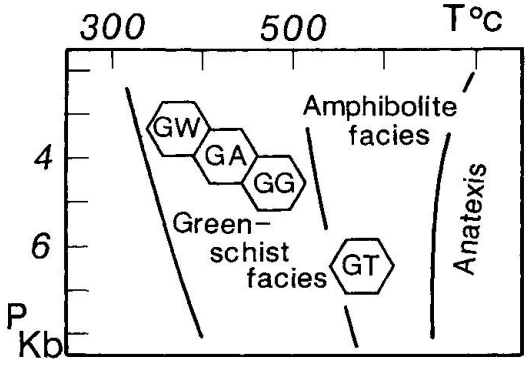

Fig. 2 Schematic PT diagram of metamorphic conditions undergone by the studied granites during Tertiary Alpine deformation. Abbreviations are the same as on figure 1.

Mineralogical changes in shear zones

In the Aar Massif, metamorphic conditions prevailing during the main deformation were in the range of 350 °C and 3 kb for the Wassen granite in the middle part of the massif, to 500 °C and 4.5 kb for the Grimsel granodiorite in the south (FREY et al., 1974, 1980; STECK, 1976; BAMBAUER and BERNOTAT, 1982; FOURCADE et al., 1989) (Fig. 2). From undeformed granite to mylonite, the grain size decreases systematically and the mineral phases change progressively across ductile shear zones leading to a fine-grained albitic mylonite. In the ultramylonite, grain size is about 30–100 μm and syntectonic reactions reflect Alpine metamorphic conditions in the Aar granite and the Grimsel granodiorite (MARQUER et al., 1985). As deformation increases, magmatic feldspars (K-feldspar, oligoclase) are replaced by an assemblage of phengite, albite and minor epidote. Abundant epidote is present in the orthogneiss but disappears in the ultramylonites. Coarse-grained magmatic biotites show a colour change from brown to green associated with rutile exsolutions forming sagenite textures. This change coincides with newly crystallized biotite at the rim of old magmatic biotite. In these shear zones, chlorite is absent. In the Wassen granite, the metamorphic paragenesis in shear zones is albite, phengite, epidote and chlorite.

The Truzzo intrusion is a two mica granite with centimetre-sized phenocrysts of K-feldspar. From weakly deformed rocks to the ultramylonite zones, strain has induced a strong ductile grain-size reduction in plagioclase and K-feldspar. In the mylonites of the Truzzo granite, ductile microstructures in plagioclase, typical of strain partitioning (BELL and JOHNSON, 1989), and the occurrence of myrmekitic textures in the K-feldspar, show high temperature conditions prevailing during Alpine deformation in this southern part of the Alps (Fig. 2). These conditions are reflected by the metamorphic paragenesis composed of recrystallized oligoclase, K-feldspar, biotite, white mica and quartz. In contrast to the newly formed inclusion-free oligoclase, the magmatic oligoclases in the weakly deformed rocks show abundant sericite inclusions. Newly recrystallized biotite has the same brown colour as the initial magmatic biotite but no sagenite textures are observed. The occurrence of recrystallized oligoclase is taken as a metamorphic indicator of amphibolite facies conditions during mylonitization (YARDLEY, 1989).

Chemical changes with increasing deformation

The use of chemical variation profiles to define chemical mass transfer in shear zones is possible only if the chemical variations associated with the initial magmatic fluctuations are below those associated with the deformation processes (see MARQUER, 1989), and if the absolute gains and losses of major and minor elements can be estimated from the comparison between mylonite and weakly deformed rocks. For the first point, recent studies performed in these shear zones have shown that the chemical modifications associated with deformation are larger than initial magmatic chemical heterogeneities (MARQUER, 1989). Besides, the magmatic trends are com-

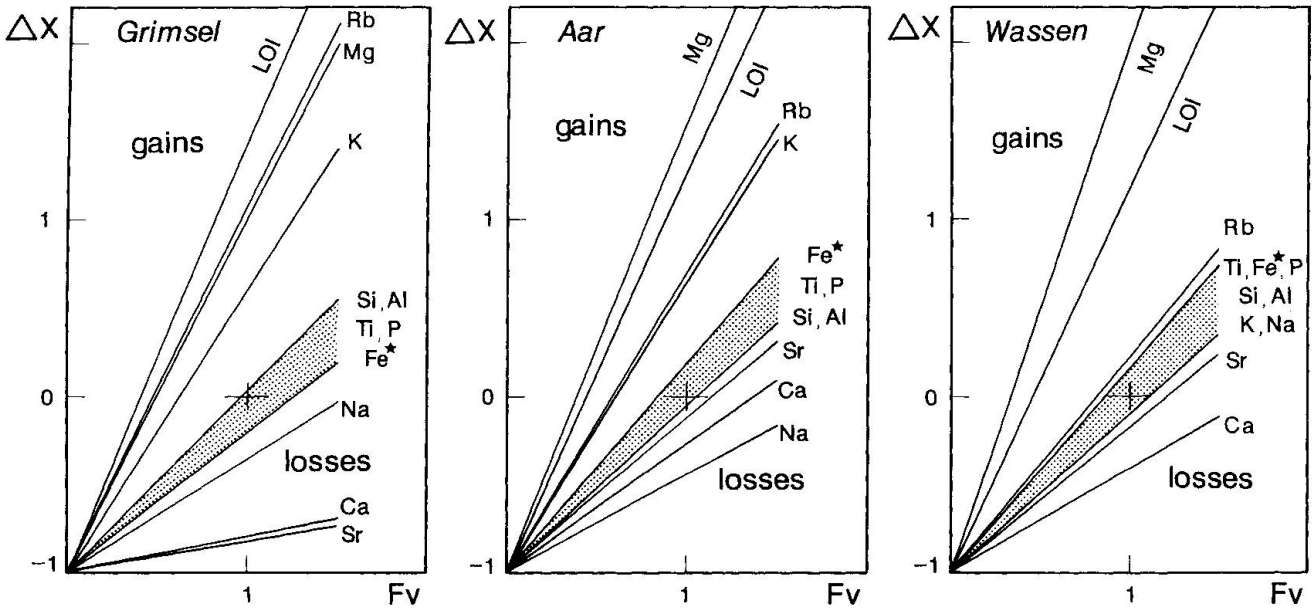

Fig. 3 Volume-composition relationships and chemical variations associated with deformation in three shear zones of the Aar massif (Grimsel, Aar, Wassen): graphical resolution of mass balance equation for the comparison of weakly deformed rocks and ultramylonites (POTDEVIN and MARQUER, 1987). Stippled area refers to immobile elements and solid lines to mobile elements. See text for explanations.

pletely different from the behaviour of mobile elements in shear zones deformed under greenschist facies conditions (see MARQUER et al., 1985; MARQUER, 1989).

For the second point, mass balance calculations cannot be expressed directly by comparison between rock analyses of the deformed rock and the initially weakly deformed rock, chosen as a magmatic reference. Estimates of absolute variations require references on volume modifications, density changes or concentrations of immobile elements. In order to compare the chemical composition of two different rocks, several methods can be used (GRESENS, 1967; GRANT, 1986; POTDEVIN and MARQUER, 1987). In this paper, the comparisons of mobile and non-mobile elements are presented by using relative mobility diagrams (Figs 3 and 4) (POTDEVIN and MARQUER, 1987). In these diagrams, the mass variation of each oxide ΔXn is normalized with respect to the content of the same oxide in the initial rock:

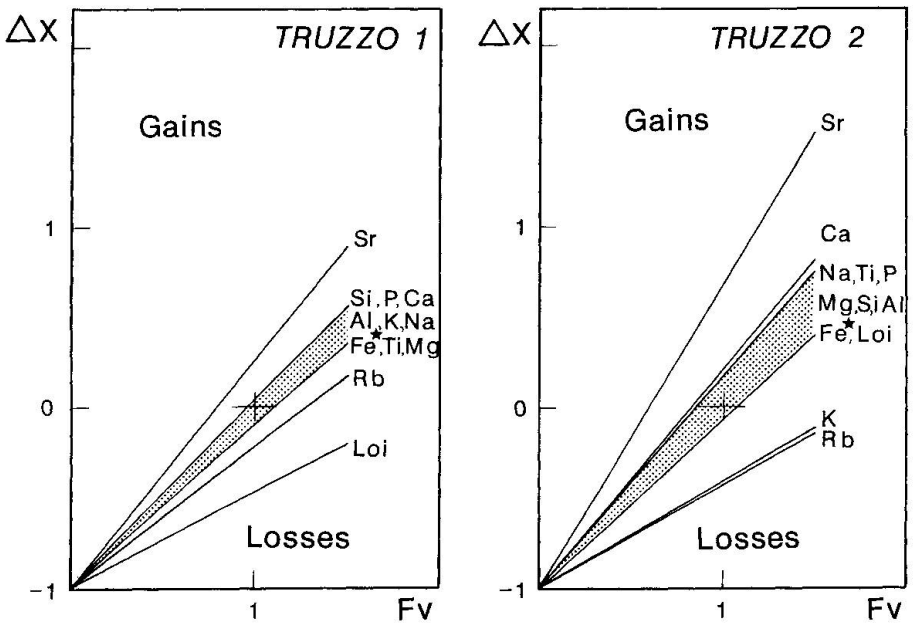

Fig. 4 Volume-composition relationships and chemical variations associated with deformation in two shear zones of the Truzzo granite. Same legend as for figure 3.

$$\Delta Xn = fv \cdot (d_{II}/d_I) \cdot (Cn_{II}/Cn_I) - 1$$

where Xn is the mass variation relative to the original mass of the element in the original rock volume, fv is given by the volume ratio between the transformed rock and undeformed precursor; d_I and d_{II}, the densities of these rocks; Cn_I and Cn_{II}, the weight percentages of the oxide n in the

initial and modified rocks, respectively. In the studied shear zones, density changes are insignificant and allow us to estimate absolute chemical mass modifications versus volume change for each oxide. These diagrams are particularly useful to compare gains and losses of major and minor elements in metagranite shear zones (MARQUER, 1989). The comparisons of major and minor elements, with significantly different concentrations in the whole rock analyses (for examples Ca, Sr, K and Rb), are facilitated by this type of diagram. The elements with similar behaviour have the same slope on the graphical solution of the equation. With this mass-balance calculation, two possibilities exist for distinguishing mobile and non-mobile elements and for calculating absolute mass transfers: calculations can be done with a fixed volume ratio or a fixed immobile element concentration.

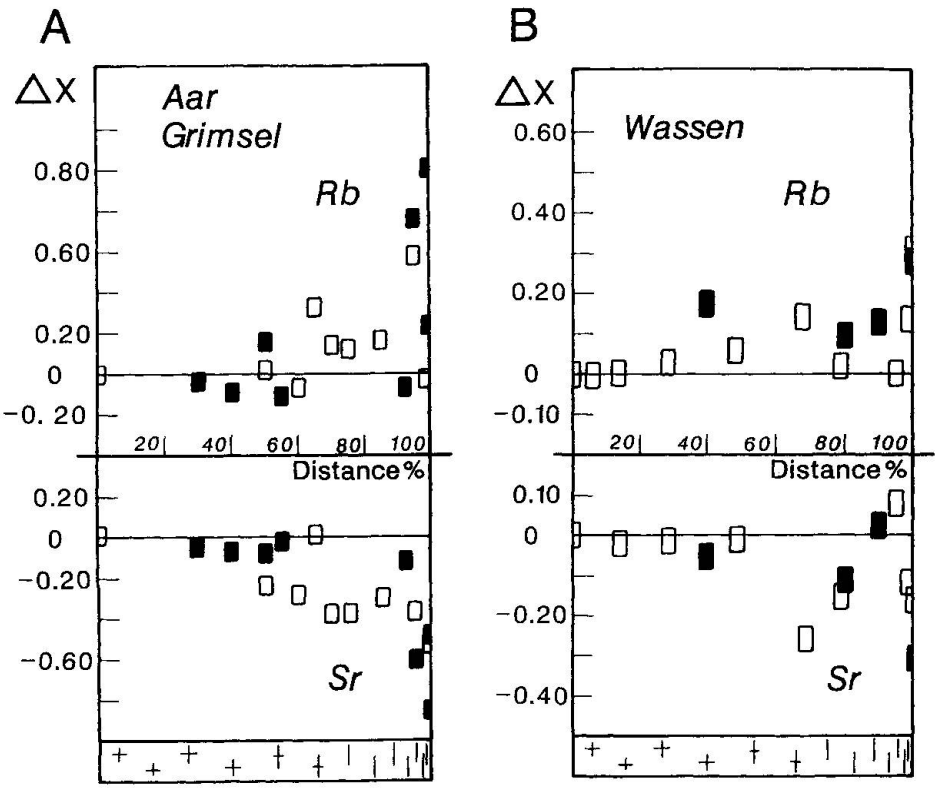

Fig. 5 Variation profiles of Rb and Sr concentrations versus normalized distance of different shear zones in the Aar massif. For each shear zone, the distance is normalized to 100. Chemical variations (ΔX) are normalized to initial concentrations of each element in the weakly deformed rocks (reference rock: point (0,0)). $\Delta X = (X-X_0)/X_0$ with X and X_0 the element concentrations in the deformed rock and the reference rock respectively. A: profiles of shear zones in the Aar granite (white dots: ACIII samples, 4 meters width, reference point ACIIIp) and the Grimsel granodiorite (black dots: ACII samples with ACIIa as reference point and AD samples with AD13 as reference point, 3 meters and 80 meters width respectively). B: profiles for two shear zones of the Wassen granite (white dots: GWC1 samples, GWC1a reference point, 10 meters; black dots: GWC3 samples, GWC3 b reference point, 1 meter). Symbol sizes are greater than analytic errors.

Assuming a fixed immobile element, as a constant aluminium abundance for example, the calculated volume changes are clearly less than 10% from undeformed precursor rocks to mylonites in all the studied shear zones (Figs 3 and 4). This very low mobility of Al_2O_3 and moderate volume changes in deformed rocks was also emphasized in several studies (CARMICHAEL, 1969; FERRY, 1979, 1982; KERRICH et al., 1977, 1980). In some of these metagranite shear zones, lacks of change in Al_2O_3 abundance and no density changes were observed (MARQUER et al., 1985). A number of weakly mobile elements with a behaviour close to Al, like Si, Ti, P and Fe*, can be identified (dashed zones on Figs 3 and 4). Based on these relatively immobile elements, deformation is assumed to take place under isovolumetric conditions (note that slight variations would not introduce any fundamental errors in mass transfer calculations). Indeed, for each comparison of the analysed concentration data between the initial magmatic rock and the deformed rocks, the mass variation ΔX of each element is calculated for a constant volume ratio fv = 1. Figures 3 and 4 summarize the results of composition-volume relationships for shear zones in greenschist facies and amphibolite facies conditions respectively. In greenschist facies mylonites (Fig. 3), a significant mobility exists for elements such as Mg, K, Rb, Na, Ca, Sr in the Grimsel granodiorite and the Aar granite. Losses of calcium, strontium and sodium in ultramylonites can be interpreted as the result of the breakdown of the feldspathic phases, while gains of K, Mg, Rb and increasing of L.O.I. reflect an increase of phengite in these deformed rocks. In the Wassen granite, however, K and Na remain immobile and only weak changes of Rb and Sr contents are recognized. These weaker chemical modifications in the Wassen shear

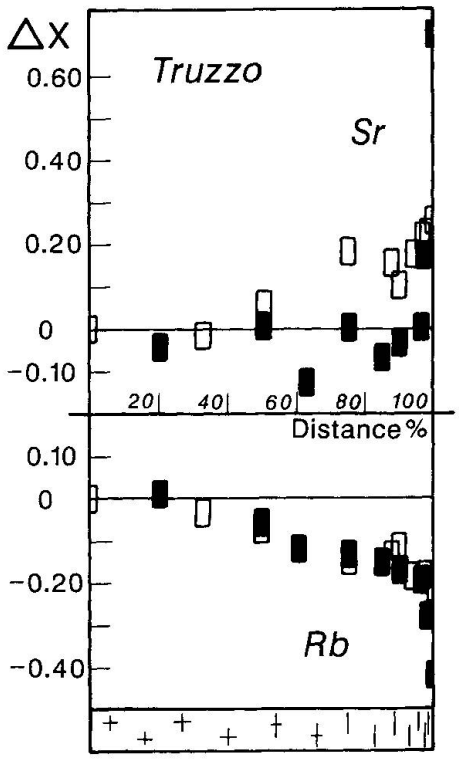

Fig. 6 Variation profiles of Rb and Sr contents versus normalized distance of two shear zones in the Truzzo granite. Same legend as in figure 5. The profiles for the shear zones are 6 meters (white dots: TC4 samples with TC4a as reference point) and 10 meters width (black dots: TC5 samples with TC5a as reference point) respectively. Symbol sizes are greater than analytical errors.

zones, can be related to the fact that deformation took place at lower thermal and pressure conditions, which is indicated by the presence of chlorite.

In the amphibolite facies, comparisons of element mobility between a weakly deformed rock and ultramylonites in two different shear zones give opposite results for the behaviour of Rb and Sr (Fig. 4). The Sr content increases with deformation while the Rb content decreases. These chemical modifications, associated with loss of K and decrease of L.O.I., can be related to the stability of K-Feldspars, the destabilization of sericite (white micas) present in undeformed plagioclases and the recrystallization of pure grains of oligoclase in ultramylonites.

In all the shear zones, the chemical variation profiles versus normalized distance emphasize the behaviour of Rb and Sr described above (Figs 5 and 6). On these profiles, the reference points (0,0) refer to the weakly deformed rocks at the margin of the shear zones. The scale of each shear zone is given in the figure captions (Figs 5 and 6) and the average weight of samples is around 4–8 kg. Even if some weak initial magmatic fluctuations disturbed slightly the relationships between chemical variations and distance, the global tendencies show a Rb increase and a Sr decrease in greenschist facies (Figs 5 a and b) and the reverse evolution in amphibolite facies (Fig. 6), whatever the scale of the shear zones. In all these shear zones, the significant chemical changes become progressively more important at the transition between orthogneiss and mylonite (MARQUER, 1989) which corresponds approximately to values greater than 60–70% on the distance axes (Figs 5 and 6). This transition corresponds to dramatic microstructural and textural modifications involving a strong reduction of grain size, a larger amount of newly recrystallized grains and a high degree of interconnected shear bands propitious to fluid circulations and mass transfers (MARQUER, 1989).

Rb–Sr isotope system

INTRUSION AGES

In the Grimsel granodiorite and the Aar granite, weakly deformed rocks have been analyzed in order to determine the magmatic age (open circles on Fig. 7). In a Rb–Sr isochron diagram, these samples define a line, which corresponds to an age of 291 ± 14 Ma and an initial isotopic ratio of 0.7054 ± 0.0005 (Fig. 7). These results are in agreement with upper Carboniferous ages for the same or for other intrusions in the Aar massif (WÜTRICH, 1965; SCHALTEGGER, 1990b; SCHALTEGGER, 1994). The low isotopic initial ratio indicates an important mantle input and low crustal contamination for these late orogenic granites (SCHALTEGGER, 1990a, 1990b).

For the Wassen granite, a magmatic age has been calculated using both new data (open circles on figure 8) and previously published data (black dots on figure 8: SCHALTEGGER, 1990b) to obtain the best estimate for the intrusion age. All these undeformed rocks define an isochron of 289 ± 19 Ma and an initial isotopic ratio of 0.7054 ± 0.0007 (Fig. 8). These results agree with the interpretation that the Wassen intrusion is a part of the large calc-alkaline to subalkaline granitic suite, the so-called Central Aar Granite, which comprises the Grimsel granodiorite and the Aar granite (LABHART, 1977; see review in SCHALTEGGER, 1994).

The age of intrusion of the Truzzo granite has been previously investigated: 339 ± 70 Ma (U/Pb zircon, GRÜNENFELDER in WEBER, 1966), 315 ± 20

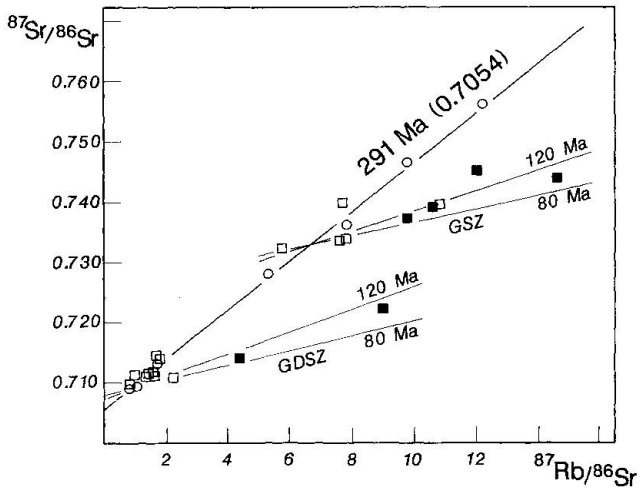

Fig. 7 Rb–Sr diagram of shear zones in the Aar granite (GSZ) and the Grimsel Granodiorite (GDSZ). Open circles: undeformed granites and granodiorites; open squares: orthogneisses; black squares: mylonites and ultramylonites. Magmatic strontium isochron is calculated from open circle samples. Both secondary isochrons are reference lines from deformed rocks in two separated shear zones (see text for explanations).

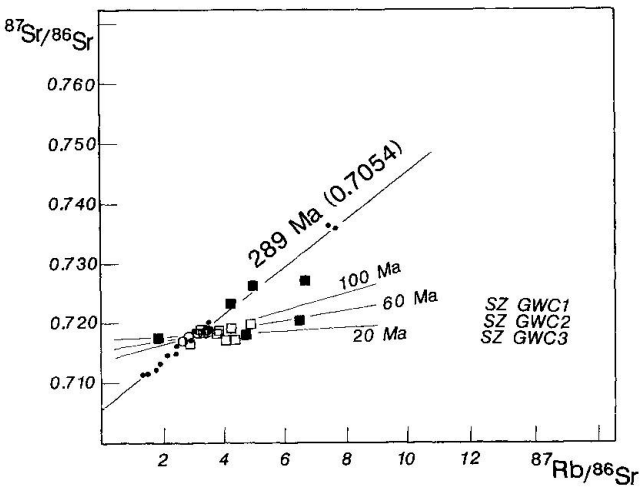

Fig. 8 Rb–Sr diagram of three shear zones in the Wassen granite (GWC1, GWC2 and GWC3) and of three independent more differentiated ultramylonites (North margin of the granite) (see Tab. 2). Open circles: weakly deformed granites; open squares: orthogneisses; black squares: mylonites and ultramylonites. Black dots: samples of weakly deformed rocks taken from SCHALTEGGER (1990b) (see Tab. 2). Magmatic Rb–Sr isochron is calculated from open circle and black dots samples. The other lines are reference model ages (see text for further explanations).

Ma (whole rock Rb–Sr: JÄGER et al., 1969; estimated error) or 303 ± 14 Ma (whole rock Rb–Sr: GULSON, 1973) (recalculated Rb–Sr whole rock ages with the new constant: $1.42 \cdot 10^{-11}$/yr). Isotope data from weakly deformed rocks published by GULSON (1973) and considered as true samples of the Truzzo granite located in the Liro valley, north of Chiavenna, were used to determine the intrusion age (black dots on Fig. 9). These isotopic data, together with new data (open circles on Fig. 9), give a line which can be interpreted in terms of intrusion age: 284 ± 21 Ma. The initial isotopic ratio is high, 0.7133 ± 0.0019 (see also GULSON [1973], p. 297), and could imply a significant crustal contribution.

Regression (YORK, 1969; BROOKS et al., 1972) yields large MSWD values which reflect the effects of Alpine metamorphism and deformation recorded by these granites.

$^{87}Sr/^{86}Sr$ ISOTOPE CHANGES DURING ALPINE DEFORMATION

The changes in Rb/Sr ratios seem well documented (see above). Nevertheless, the possibility that some changes occurred in the $^{87}Sr/^{86}Sr$ ratios has to be considered. Prior to any examination of such isotopic alteration, it is necessary to demonstrate that the deformed rock is derived from a pristine granitic rock with a uniform and similar isotopic composition and Rb/Sr ratio. This undeformed rock is considered as the magmatic reference in each individual shear zone.

From the Aar granite, in the shear zone GSZ (Fig. 7, Tab. 1), we can observe that the undeformed samples, close to the studied shear zone, (Aar3–6) and weakly deformed ones (ACIIIa–p) exhibit lower $^{87}Sr/^{86}Sr$ ratios (range between 0.726 and 0.733: recalculated at the Oligocene time of the shearing) than the mylonitic samples (ACIIIg–i: 0.734 to 0.741). The samples Aar1–2 are far from this shear zone and correspond to undeformed granites with higher SiO_2 content (74.50–76.50%) than Aar3–6 or ACIIIa–p (SiO_2 < 74.50%). The same evolution is observed for the granodiorite samples (GDSZ, Fig. 7). The undeformed and weakly deformed rocks (open circles, Fig. 7) were collected at a scale larger than one kilometer. On the isochron diagram, these samples show varying Rb/Sr ratios due to magmatic differentiation (MARQUER et al., 1985). On the other hand, the deformed samples from the granitic and granodioritic shear zones (GSZ and GDSZ) were collected at the metre-decametre scale. In the same isochron diagram, they form two different arrays with positive slopes (open and black squares, Fig. 7). Moreover, the different types of chemical changes related to the magmatic evolution or to the modifications associated

with deformation are also well constrained by the analyses of major elements, minor elements and stable isotopes (MARQUER, 1989; FOURCADE et al., 1989).

For each shear zone studied, these last observations strongly suggest that before deformation, the actually deformed rock had a Rb/Sr ratio close to that of the undeformed reference rock. Consequently, the observed increase of the $^{87}Sr/^{86}Sr$ ratio for mylonite rocks is induced by mass transfer during deformation under greenschist facies conditions. Strontium isotope compositions also change within the amphibolite facies shear zones (Fig 9), but in the opposite sense: a decrease of $^{87}Sr/^{86}Sr$ ratios is observed in deformed rocks.

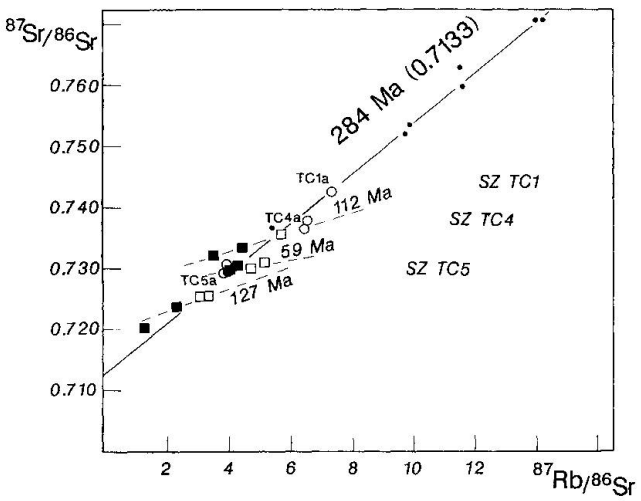

Fig. 9 Rb–Sr diagram of three shear zones in the Truzzo granite (TC1, TC4 and TC5). Open circles: weakly deformed granites; open squares: orthogneisses; black squares: mylonites and ultramylonites. Black dots: samples of weakly deformed rocks taken from GULSON (1973) (see Tab. 3). Initial Rb–Sr isochron is calculated from open circle and black dots samples. The three dashed lines are reference model ages for three different shear zones (see text for explanations).

EFFECTS OF METAMORPHISM AND DEFORMATION ON THE Rb-Sr ISOCHRON DIAGRAM

In greenschist facies, the Rb/Sr and Sr isotope ratios increase significantly in the ultramylonites from initial values close to those of the isochron (Figs 7 and 8). The scattered values for deformed rocks on the right-hand part of the magmatic isochron do not show a random distribution but yield linear arrays from initially weakly deformed granites to ultramylonites. For each individual shear zone, these lines could be interpreted in terms of ages of geological events between 80 and 120 Ma for the Aar granite and the Grimsel granodiorite or around 60 Ma for the Wassen granite. Because these syntectonic shear zones are interpreted to be Oligocene, on the basis of stratigraphy-tectonic relationships and cooling ages (see geological setting and timing of Alpine deformation), the apparent age results are meaningless. These lines only reflect the chemical modifications of the Rb–Sr system during progressive deformation and metamorphism of the granites.

In amphibolite facies, Rb/Sr and Sr isotope ratios decrease. The mylonites and ultramylonites are offset to the left of the initial isochron (Fig. 9). Three shear zones are presented and they show less variations than in the greenschist facies. For each shear zone, the deviation of analyses of deformed rocks is rather small and leaves these data close to the initial isochron. Due to the small shift observed on the Rb–Sr system it is not possible to calculate "isochron ages". Nevertheless, reference trends from the orthogneiss and mylonites may be calculated of around 127, 112 and 59 Ma. They are interpreted as spurious ages because the main ductile deformation is post-Eocene (e.g.: nappe emplacement over Eocene flysch sediments [SCHMID et al., 1990]) and because there is evidence for chemical mass-transfer (Fig. 6) and open system behaviour for Rb and Sr in the metagranite shear zones.

Discussion

As demonstrated above, the major effects of chemical mass-transfer, metamorphism and deformation occur in mylonites and ultramylonites. These effects are responsible for structural and textural changes in deformed rocks, such as the grain size reduction and the high degree of interconnected shear bands, which increase the reaction surfaces of minerals and the fluid path-ways respectively (MARQUER, 1989). Temperature conditions control both the types of deformation mechanisms and the metamorphic paragenesis in retrograde deformed granitic rocks. At the grain scale, deformation and recrystallization mechanisms such as diffusion, dislocation glide and dislocation creep, are increasingly active at higher temperature (TULLIS and YUND, 1987; see review in BELL and JOHNSON, 1989, p. 159). The granitoids studied consist on average of 60% feldspar. With such a high percentage, deformation of the feldspathic phases strongly influences the mechanical and rheological behaviour of the bulk

rock (GAPAIS, 1989). All the initial magmatic feldspathic phases observed in the Truzzo granite show ductile deformation and recrystallization of grains of K-feldspar and oligoclase, while in the Aar massif, deformation of initial K-feldspar and oligoclase is brittle-ductile and crystallization of a new assemblage of albite-phengite increases progressively with strain intensity (MARQUER, 1989). The stable initial assemblage in metagranite shear-zones deformed in amphibolite facies controls the low chemical mobility of major and minor elements and the small modification of the Rb–Sr system (Fig. 4). In contrast, the large chemical variations recorded by shear zones in the Aar massif can be explained by the brittle-ductile deformation allowing fluid circulation and enhancing retrograde metamorphism (albite-phengite assemblage). The different chemical behaviour of metagranite shear zones at the transition between amphibolite and greenschist facies is emphasized by these previous examples. In greenschist facies, the deformation is preferentially controlled by fluid-assisted deformation mechanisms and is associated with retromorphic reactions. Whereas in amphibolite facies, intracrystalline mechanisms are prevailing and the initial paragenesis is stable (MARQUER, 1989).

If the results of chemical mass-transfer and combined mineralogical variations during deformation processes explain the increase (or decrease) of the Rb/Sr ratio, an explanation must be found to justify the increase (or decrease) of the $^{87}Sr/^{86}Sr$ ratio in mylonites with respect to the initial parent-rocks. The results of isotopic modifications in shear zones can be summarized as follows: (i) a decrease of the $^{87}Sr/^{86}Sr$ ratios in amphibolite facies, (ii) an increase of the $^{87}Sr/^{86}Sr$ ratios in greenschist facies. These different types of change in strontium isotope composition during deformation at different levels of the continental crust reflect the lack of a unique and large continental fluid circulation (MARQUER and BURKHARD, 1992). Indeed, these isotope ratios are an argument against systematic homogeneous composition for eventual large fluid contaminations in the upper and middle crust, which would be responsible for identical isotopic modifications in the deformed zones. In particular, if the $^{87}Sr/^{86}Sr$ changes were exclusively related to external radiogenic Sr introduced into the system by fluid circulation, the crustal Sr-enriched fluids would have had to be very heterogeneous in isotope composition to explain the opposite variations observed in greenschist and amphibolite facies. This external fluid would have had high isotope signature to explain changes in the Aar granite where magmatic Sr isotope ratios were already high at the time of metamorphism. The intermediate range of fluid fluxes calculated for the shear zones of the Grimsel granodiorite ($5 \cdot 10^4$ moles/cm^2) emphasizes that the metasomatism in these deformation zones does not require large-scale circulations of chemically exotic fluids (DIPPLE and FERRY, 1992).

Here, three different models assuming a small influence of external fluids are presented (Fig. 10):

In a first model, all the minerals were in isotope equilibrium during the shearing processes. Magmatic biotite and feldspar were totally reset and as observed, new crystallization of phengite produced a significant increase of the Rb/Sr ratio in the mylonitic and ultramylonitic facies compared to the undeformed rock (Fig. 10a). Even if chemical mass-transfers occur, the "deformed rock-source rock" line reflects complete isotope homogenization of mineral phases and produces an isochron relationship. In the studied cases, calculated ages would have to be Oligocene or younger with respect to geological data. The failure of this theoretical model reflects the lack of total homogenization, undoubtedly due to the low temperature and the lack of bulk equilibration at the scale of the shear zones.

In the second hypothesis, only the Rb/Sr ratios are increased during shearing. Indeed, in the isochron diagram, the deformed rocks (WRsz) exhibit systematically higher $^{87}Sr/^{86}Sr$ ratios than their corresponding undeformed precursors (big stars on Fig. 10b). The main difference between model I and model II is that there was not the same composition before shearing between the rocks that were to become sheared and those that were not. This hypothesis implies a systematically more differentiated chemical character for deformed rocks. This assumption is in disagreement with petrological and geochemical data which support that the shear zones are developed from the same initial rocks as those actually found in preserved lenses (MARQUER et al., 1985; MARQUER, 1989). Furthermore, this model does not explain the opposite behaviour in the amphibolite facies shear zones from the Truzzo granite in which the most deformed rocks have the lowest Rb/Sr ratios and would be, in that case, the "less differentiated" rocks.

The third model combines both Rb/Sr and $^{87}Sr/^{86}Sr$ changes and is based on an open system associated with progressive deformation and mineralogical changes in shear zones (BIELSKI et al., 1979) (Fig. 10c). These changes correspond to newly crystallized minerals and progressive disappearance of some magmatic relics in which the initial isotopic signature is partly preserved. This phenomenon is also described from shear zones

in the central Pyrenees (MAJOOR, 1988). The whole rock composition of the future mylonite is close to the isotopic and chemical ratios displayed by the weakly deformed rocks (stars on Fig. 10c). In the studied shear zones, isotope composition of mylonite can correspond to a mixing between new mineral phases and partly preserved magmatic minerals with high $^{87}Sr/^{86}Sr$ compositions. The progressive and partial transformations from oligoclase-K-feldspar and magmatic biotite bearing granites to phengite-albite and secondary biotite bearing mylonites can explain the continuous behaviour of Rb–Sr systematics in shear zones which have suffered greenschist facies deformation (Fig. 10c). In this model, the shift of $^{87}Sr/^{86}Sr$ ratios and the lines defined by shear zone samples correspond to spurious ages governed in part by the isotopic composition of pre-existing mineral relics, mainly magmatic biotite. In particular, the recrystallized biotites in the basement rocks of the Aar massif maintain inherited isotopic compositions and give old mixing ages with respect to Tertiary events (DEMPSTER, 1986). Thus, the difference in $^{87}Sr/^{86}Sr$ ratios between mylonites (black squares), orthogneisses (open squares) and original rocks (stars) corresponds to different mineral proportions. With this model, the spurious apparent ages produced have to be between the original rock age and the age of shearing. This last model can also explain the slight decrease of $^{87}Sr/^{86}Sr$ ratios and the existence of mylonites with Rb/Sr and Sr isotopic ratios close to the magmatic isochron in the case of amphibolite facies shear zones. The slight chemical and isotopic fluctuations are related to the stability of the initial paragenesis in both deformed and weakly deformed rocks. Furthermore the influence of a partly preserved magmatic phases, in this case, plagioclase with low isotope composition, may also explain the decrease of the observed isotope ratio for mylonites deformed under amphibolite facies conditions.

Conclusions

The magmatic ages, well-preserved in weakly deformed rocks from Truzzo granite and different granites of the Aar massif, emphasize the heterogeneous type of the deformations preferentially localized in narrow shear zones. Except for amphibolite shear zones, orthogneisses and mylonites developed in greenschist facies show large scatter in Rb–Sr ages. In the greenschist facies shear zones deformation enhanced metamorphic reactions and increased the fluid path-ways by grain size reduction. However, metamorphic con-

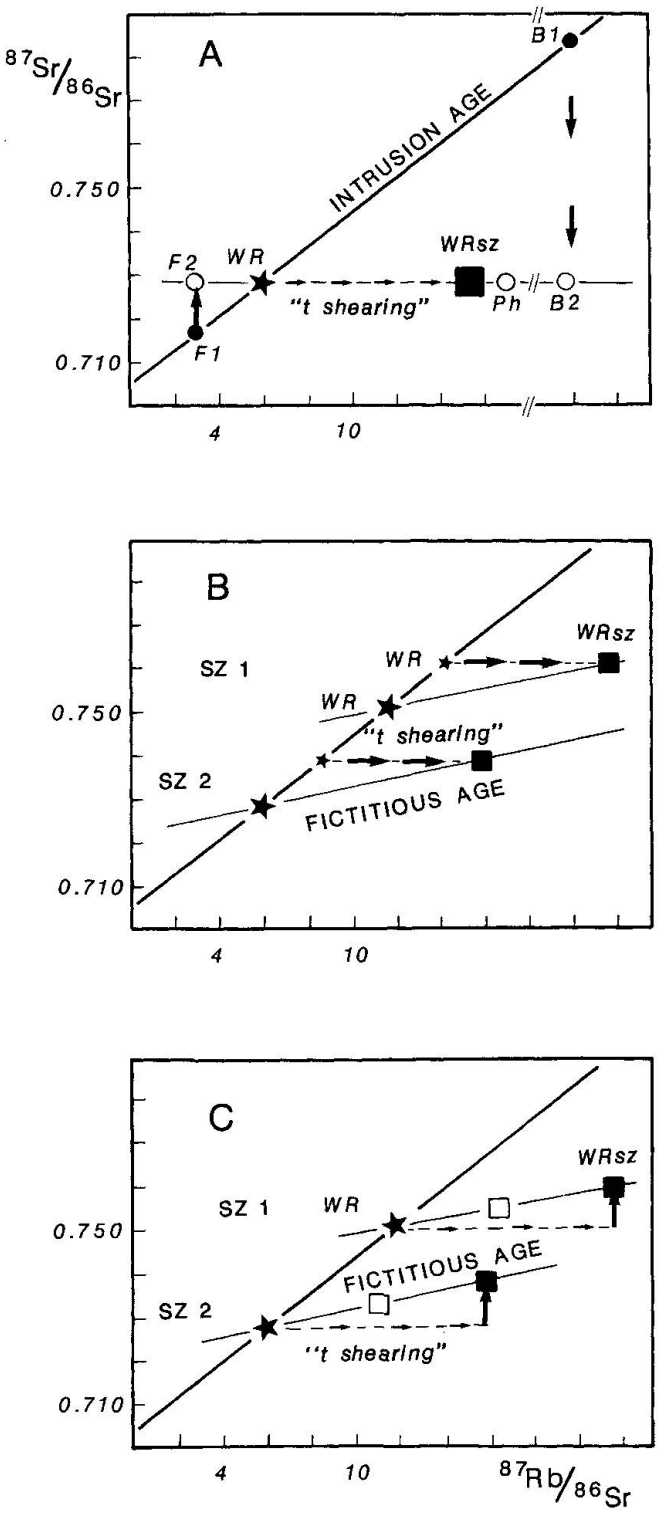

Fig. 10 Different schematic interpretations for the behaviour of whole rocks isotopic compositions of mylonites in the Rb–Sr diagrams. In all diagrams, WR (stars) and WRsz (black squares) are respectively whole rock composition of the undeformed rocks and ultramylonites. A: initial magmatic minerals (black dots): feldspath (F1), biotite (B1); new metamorphic minerals (open circles): feldspath (F2), biotite (B2) and phengite (Ph). "t shearing" means time of deformation. Further explanations in text.

ditions control mineral reactions and element mobilities. For example, in greenschist facies shear zones, the breakdown of feldspars and crystallization of albite-phengite assemblages implies an increase in the Rb/Sr ratio of the whole rock system in mylonites while weak chemical modifications occurred in amphibolite shear zones in which the magmatic paragenesis was stable during deformation. These results emphasize that the Rb–Sr whole rock dating method is not well suited to estimate directly the age of heterogeneous deformation in granitic rocks which have undergone low grade metamorphism. Two essential reasons can be pointed out: first, the presence of shear bands and local preserved domains imply an heterogeneous isotopic composition at a smaller scale than the samples. Second, isotopic homogenization postulated in high-grade metamorphic shear zones is controlled by diffusion processes. The diffusion mechanism is thermally enhanced and for greenschist facies conditions of the Aar massif, a bulk isotopic homogenization was, with no doubt, never reached. Radiometric method alone never has solved an Alpine problem, and this last point underlines the caution that must be taken when using and interpreting Rb–Sr whole rock ages of deformed rocks in different part of the mountain chains.

A listing of all the major and minor element analyses in these different shear zones is available (contact D. Marquer).

Acknowledgements

This research was supported by the Swiss National Foundation projects FNSRS No 20-26.313-89. We thank H.R. Pfeifer (Lausanne) for the logistical support of all aspects of chemical analysis. The critical review of Jan Kramers was very valuable to improve the last version of this manuscript. Our colleagues in the CAESS Rennes and Neuchâtel are particularly acknowledged.

References

ABBOTT, J.T. (1972): Rb–Sr study of isotopic redistribution in a Precambrian mylonite-bearing Shear zone, Northern Front Range, Colorado. Geol. Soc. Amer. Bull., 83, 487–494.

ABRECHT, J. (1994): Geologic units of the Aar massif and their pre-alpine rock associations: a critical review. Schweiz. Mineral. Petrogr. Mitt., 74/1, 5–28.

BAMBAUER, H.V. and BERNOTAT, W.H. (1982): The microcline/sanidine transformation isograd in metamorphic regions. Schweiz. Mineral. Petrogr. Mitt., 62, 185–230.

BAROVICH, K.M. and PATCHETT, P.J. (1992): Behavior of isotopic systematics during deformation and metamorphism: a Hf, Nd and Sr isotopic study of mylonitized granite. Contrib. Mineral. Petrol., 109, 386–393.

BELL, T.H. and JOHNSON, S.E. (1989): The role of deformation partitioning in the deformation and recrystallization of plagioclase and K-feldspar in the Woodroffe Thrust mylonite zone, central Australia. J. Metam. Geol., 7, 151–168.

BICKLE, M.J. and MCKENZIE, D.P. (1987): The transport of heat and matter by fluids during metamorphism. Contrib. Mineral. Petrol., 95, 384–392.

BIELSKI, M., JÄGER, E. and STEINITZ, G. (1979): The geochronology of Iqua Granite (Wadi Kid Pluton), southern Sinai. Contrib. Mineral. Petrol., 70, 159–165.

BOSSIÈRE, G. (1980): Un complexe métamorphique poly-cyclique et sa blastomylonitisation. Etude pétrologique de la partie occidentale du massif de grande Kabylie. Unpubl. Thesis, University of Nantes, Nantes.

BREITSCHMID, A. (1982): Diagenese und schwache Metamorphose in den sedimentären Abfolgen der Zentralschweizer Alpen (Vierwaldstättersee, Urirotstock). Eclog. geol. Helv., 75/2, 331–380.

BROOK, C., HART, S.R. and WENDT, I. (1972): Realistic use of two error regression treatments as applied to rubidium-strontium data. Reviews in Geophysic and Space Physic, 10/2, 551–557.

BRODIE, K.H. and RUTTER, E.H. (1985): On the relationship between deformation and metamorphism with special reference to the behaviour of basic rocks. In: Kinetics, textures and deformation (Advances in physical geochemistry, volume 4), eds THOMPSON, A.B. and RUBIE, D.C., pp. 138–179. Springer-Verlag, New-York.

CARMICHAEL, D.M. (1969): On the mechanism of prograde metamorphic reactions in quartz bearing pelitic rocks. Contrib. Mineral. Petrol., 20, 244–267.

CHOUKROUNE, P. and GAPAIS, D. (1983): Strain pattern in the Aar granite (Central Alps); Orthogneiss developed by bulk inhomogeneous flattening. J. Struct. Geol., 5 3/4, 411–418.

DEMPSTER, T.J. (1986): Isotope systematics in minerals: biotite rejuvenation and exchange during alpine metamorphism. Earth Planet. Sci. Lett., 78, 355–367.

DEUTSCH, A. and STEIGER, R.H. (1985): Hornblende K–Ar and the climax of tertiary metamorphism in the Lepontine Alps (South Central Switzerland); an old problem reassessed. Earth Planet. Sci. Lett., 72, 175–189.

DIETRICH, R.V., FULLAGAR, P.D. and BOTTINO, M.L. (1969): K/Ar and Rb/Sr dating of tectonic events in the Appalachian of Southwestern Virginia. Geol. Soc. Amer. Bull., 80, 307–314.

DIPPLE, G.M., WINTSCH, R.P. and ANDREWS, M.S. (1990): Identification of the scales of differential element mobility in a ductile fault zone. J. Metam. Geol., 8, 645–661.

DIPPLE, G.M. and FERRY, J.M. (1992): Metasomatism and fluid flow in ductile fault zones. Contrib. Mineral. Petrol., 112, 149–164.

ETHERIDGE, M.A. and COOPER, J.A. (1981): Rb/Sr isotopic and geochemical evolution of a recristallized shear (mylonite) zone at Broken Hill. Contrib. Mineral. Petrol., 78, 74–84.

ETHERIDGE, M.A., WALL, V.J. and VERNON, R.H. (1983): The role of the fluid phase during regional metamorphism and deformation. J. Metam. Geol., 1, 205–226.

ETHERIDGE, M.A., WALL, V.J., COX, S.F. and VERNON, R.H. (1984): High fluid pressures during regional metamorphism and deformation: Implications for mass transport and deformation mechanisms. J. Geophys. Res., 89B (6), 4344–4358.

FERRY, J.M. (1979): Reaction mechamisms, physical conditions, and mass transfer during hydrothermal alteration of mica and feldspar in granitic rocks from South Central Maine, USA. Contrib. Mineral. Petrol., 68, 125–139.

FERRY, J.M. (1982): A comparative geochemical study of pelitic schists and metamorphosed carbonates rocks from South Central Maine, USA. Contrib. Mineral. Petrol., 80, 59–72.

FERRY, J.M. and DIPPLE, G. (1991): Fluid flow, mineral reactions, and metasomatism. Geology, 19, 211–214.

FOURCADE, S., MARQUER, D. and JAVOY, M. (1989): $^{18}O/^{16}O$ variations and fluid circulation in a deep shear zone: the case of the alpine ultramylonites from the Aar massif (Central Alps, Switzerland). Chemical Geology, 77, 119–131.

FREY, M., BUCHER, K., FRANK, E. and MULLIS, J. (1980): Alpine metamorphism along the geotraverse Basel–Chiasso: a review. Eclogae geol. Helv., 73/2, 527–546.

FREY, M., HUNZIKER, J.C., FRANK, W., BOCQUET, J., Dal PIAZ, G.V., JÄGER, E. and NIGGLI, E. (1974): Alpine metamorphism of the Alps: a review. Schweiz. Mineral. Petrogr. Mitt., 54/2/3, 277–290.

FYFE, W.S., PRICE, N.J. and THOMPSON, A.B. (1978): Fluids in the Earth crust. 383 p., Elsevier, Amsterdam.

GAPAIS, D., BALE, P., CHOUKROUNE, P., COBBOLD, P., MAHDJOUB, Y. and MARQUER, D. (1987): Bulk kinematics from shear zone patterns; some field examples. J. Struct. Geol., 9 5/6, 635–646.

GAPAIS, D. (1989): Shear structures within deformed granites: Mechanical and thermal indicators. Geology, 17, 1144–1147.

GRANT, J.A. (1986): The isocon diagram – a simple solution to Gresens' equation for metasomatic alteration. Economic Geology, 81, 1976–1982.

GRESENS, R.L. (1967): Composition-volume relationships of metasomatism. Chemical Geology, 2, 47–65.

GULSON, B.L. (1973): Age relations in the Bergell region of the South-East Swiss Alps: With some geochemical comparisons. Eclogae geol. Helv., 66/2, 293–313.

HARPER, C.T. and LANDIS, C.A. (1967): K–Ar ages from regionally metamorphosed rocks, South Island, New Zealand, and some tectonic implications. Earth Planet. Sci. Lett., 5, 413–422.

HICKMANN, M.H. (1984): Rb–Sr chemical and isotopic response of gneisses in late Archean shear zones of the Limpopo Mobile belt, Southern Africa. Precambrian Res., 24, 123–130.

HUNZIKER, J.C. (1970): Polymetamorphism in the Monte Rosa, Western Alps. Eclogae geol. Helv., 63/1, 151–161.

HURFORD, A., FLISCH, M. and JÄGER, E. (1989): Unravelling the thermo-tectonic evolution of the Alps: a contribution from fission track analysis and mica dating. In: Alpine Tectonics (eds COWARD, M., DIETRICH, D. and PARK, R.G.), pp. 369–398. Geological Society Special Publication, 45, London.

JÄGER, E., HUNZIKER, J.C. and GRAESER, ST. (1969): Colloquium on the geochronology of phanerozoic orogenic belts. Unpubl. Geochronology congress Report and field trip guide book.

JÄGER, E., NIGGLI, E. and WENK, E. (1967): Altersbestimmungen an Glimmern der Zentralalpen. Beiträge zur Geologischen Karte der Schweiz, 134, 1–67.

KERRICH, R., FYFE, W.S., GROMANN, B.E. and ALLISON, L. (1977): Local modification of rock chemistry by deformation. Contrib. Mineral. Petrol., 65, 183–190.

KERRICH, R., ALLISON, I., BARNETT, R.L., MOSS, S. and STARKEY, J. (1980): Microstructural and chemical transformations accompanying deformation of granite in a shear zone at Miéville, Switzerland; with implications for stress corrosion cracking and superplastic flow. Contrib. Mineral. and Petrol., 73, 221–242.

KERRICH, R., LATOUR, T.E. and WILLMORE, L. (1984): Fluid participation in deep fault zones: evidence from geological, geochemical and $^{18}O/^{16}O$ relations. J. Geophys. Res., 89, 4331–4343.

LABHART, T.P. (1977): Aarmassiv und Gotthardmassiv. Sammlung Geologischer Führer, Band 63. Gebrüder Borntraeger, Berlin, Stuttgart.

MCCAIG, A.M. (1984): Fluid-rock interaction in some shear zones from the central Pyrenees. Journal of Metamorphic Geology, 2, 129–141.

MCCAIG, A.M. (1989): Fluid flow through fault zones. Nature, 340, 600.

MCCAIG, A.M., WICKHAM, S.M. and TAYLOR, H.P. (1990a): Deep fluid circulation in Alpine shear zones, Pyrenees, France: field and oxygen isotope studies. Contrib. Mineral. Petrol., 106, 41–60.

MCCAIG, A.M. and KNIPE, R.J. (1990b): Mass-transport mechanism in deforming rocks: recognition using microstructural and microchemical criteria. Geology, 18, 824–827.

MAJOOR, F.J.M. (1988): A geochronological study of the axial zone of the central Pyrenees, with emphasis on Variscan events and Alpine resetting. Unpubl. Ph. D. Thesis, Isotopen-Geologie Amsterdam.

MARQUER, D. (1989): Transfert de matière et déformation des granitoïdes – Aspects méthodologiques. Schweiz. Mineral. Petrogr. Mitt., 69, 13–33.

MARQUER, D. (1991): Structures et cinématique des déformations alpines dans le granite de Truzzo (Nappe de Tambo: Alpes centrales suisses). Eclogae geol. Helv., 84/1, 107–123.

MARQUER, D. and GAPAIS, D. (1985): Les massifs cristallins externes sur une transversale Guttanen-Val Bedretto (Alpes Centrales): Structures et histoire cinématique. Comptes Rendus de l'Académie des Sciences de Paris, 301/II/8, 543–546.

MARQUER, D., GAPAIS, D. and CAPDEVILA, R. (1985): Comportement chimique et orthogneissification d'une granodiorite en faciès schistes verts (Massif de l'Aar, Alpes centrales suisses). Bul. Miner., 108, 209–221.

MARQUER, D. and BURKHARD, M. (1992): Fluid circulation, progressive deformation and mass-transfer processes in the upper crust: example of basement-cover relationships in the External Cristalline Massifs (Switzerland). J. of Struct. Geol., 8/9, 1047–1059.

MARQUER, D., BAUDIN, TH., PEUCAT, J.J. and PERSOZ, F. (1993): Rb–Sr mica ages in the Alpine shear zones of the Truzzo granite: Timing of the Tertiary Alpine P-T-deformations in the Tambo nappe (Central Alps, Switzerland). Eclogae geol. Helv., 85/3, 1–61.

MERCOLLI, I., ABRECHT, J. and BIINO, G. (1994): The pre-Alpine crustal evolution of the Aar-, Gotthard- and Tavetsch massifs. Schweiz. Mineral. Petrogr. Mitt., 74/1, 3–4.

PEUCAT, J.J. (1983): Géochronologie des roches métamorphiques (Rb–Sr et U–Pb). Exemples choisis au Groënland, en Laponie dans le Massif Armoricain

et en Grande Kabylie. Mémoires de la Société Mineralogique de Bretagne, 28, 158 pp.

PFIFFNER, O.A. (1986): Evolution of the north alpine foreland basin in the Central Alps. Special Publications International Association of Sedimentologists, 8, 219–228.

POTDEVIN, J.L. and MARQUER, D. (1987): Méthodes de quantification des transferts de matière par les fluides dans les roches métamorphiques déformées. Geodinamica Acta, 1/3, 193–206.

RUMBLE, D. (1989): Evidences of fluid flow during regional metamorphism. Eur. J. Miner., 1, 731–737.

SCHALTEGGER, U. (1990a): The Central Aar granite: Highly differenciated calc-alkaline magmatism in the Aar Massif (Central Alps, Switzerland). Eur. J. Miner., 2, 245–259.

SCHALTEGGER, U. (1990b): Post-magmatic resetting of Rb–Sr whole rock ages – a study in the Central Aar Granite (Central Alps, Switzerland). Geologische Rundschau, 79/3, 709–724.

SCHALTEGGER, U. (1994): Unravelling the pre-Mesozoic history of the Aar and Gotthard massifs (Central Alps) by isotopic dating – a review. Schweiz. Mineral. Petrogr. Mitt., 74/1, 41–52.

SCHMID, S.M., RÜCK, P. and SCHREURS, G. (1990): The significance of the Schams nappes for the reconstruction of the paleotectonic and orogenic evolution of the Penninic zone along the NFP 20-East traverse (Grisons, Eastern Switzerland). Mémoires de la Société Géologique Suisse, 1, 263–287.

SELVERSTONE, J., MORTEANI, G. and STAUDE, J.M. (1991): Fluid channelling during ductile shearing: transformation of granodiorite into aluminous schist in Tauern Window, Eastern Alps. J. of Metam. Geol., 9, 419–431.

SINHA, A.K., HEWITT, D.A. and RIMSTIDT, J.D (1986): Fluid interaction and element mobility in the development of ultramylonites. Geology, 14, 883–886.

STECK, A. (1966): Petrographische und Tektonische Untersuchungen am Zentralen Aaregranit und seinen altkristallinen Hüllgesteinen im westlichen Aarmassiv. Beiträge zur Geologischen Karte der Schweiz, 130, 99 pp.

STECK, A. (1976): Albit-Oligoklas-Mineralgesellschaften der Peristeritlücke aus alpinmetamorphen Granitgneisen des Gotthardmassivs. Schweiz. Mineral. Petrogr. Mitt., 56, 269–292.

STEIGER, R.H. (1964): Dating of orogenic phases in the Central Alps by K–Ar ages of Hornblende. J. of Geophys. Res., 69/24, 5407–5421.

STEINER, H. (1984): Radiometrische Altersbestimmungen an Gesteinen der Maggia-Decke (Pennikum der Zentral-Alpen). Schweiz. Mineral. Petrogr. Mitt., 64, 227–259.

STEINITZ, G. and JÄGER, E. (1981): Rb–Sr and K–Ar studies on rocks from the Suretta nappe; Eastern Switzerland. Schweiz. Mineral. Petrogr. Mitt., 61, 121–131.

THÖNI, M. (1983): The thermal climax of the early Alpine metamorphism in the Austroalpine thrust sheet. Memorie di Scienze Geologiche di Padova, 36, 211–238.

THÖNI, M. (1986): The Rb–Sr Thin slab isochron method – an unreliable geochronologic method for dating geologic events in polymetamorphic terrains? Evidence from the Austroalpine basement nappe, the eastern Alps. Memorie di Scienze Geologiche di Padova, 38, 283–352.

TOBISCH, O.T., BARTON, M.D. and VERNON, R.H. (1991): Fluid-enhanced deformation: transformation of granitoids to banded mylonites, western Sierra Nevada, California, and southeastern Australia. J. Struct. Geol., 13/10, 1137–1156.

TRÜMPY, R. (1980): Geology of Switzerland, a guide book. Part A: An Outline of the Geology of Switzerland. eds Schweizerische Geologische Kommission, 104 pp. Wepf, Basel.

TULLIS, J. and YUND, R.A. (1987): Transition from cataclastic flow to dislocation creep of feldspar: Mechanism and microstructures. Geology, 15, 606–609.

WEBER, W. (1966): Zur Geologie zwischen Chiavenna und Mesocco. Mitteilungen aus dem Geologischen Institut der Eidg. Techn. Hochschule und der Universität Zürich, 57, 248 pp.

WINSOR, C.N. (1984): Solution transfer syn-S2: an inferred means of deriving fault fill in the Lake Moondarra area, Mt Isa, Queensland, Australia, based on oxygen isotope results. J. Struct. Geol., 6, 679–685.

WÜTHRICH, H. (1965): Rb-Sr-Altersbestimmungen am alpinmetamorph überprägten Aarmassiv. Schweiz. Mineral. Petrogr. Mitt., 45, 875–971.

YARDLEY, B.W.D. (1989): An Introduction to Metamorphic Petrology. Longman Earth science series, Essex, 248 pp.

YORK, D. (1969): Least squares of straight line with correlated errors. Earth Planet. Sci. Lett., 5, 320–324.

Manuscript received June 20, 1994; revision accepted August 25, 1994.

Appendix

Rb and Sr contents were determined by XRF method in Géosciences Rennes and the University of Lausanne. Isotope analyses were performed in Rennes using a Cameca THN 206 and a Finnigan Mat 262 mass spectrometer. NBS standard 987 yielded values of 0.71020 ± 5. Uncertainties for $^{87}Rb/^{86}Sr$ ratios were 2%. Isochrons were calculated according to the method of York (1969). The probable errors of the isochrons are quoted as $2s \cdot \sqrt{MSWD}$, where MSWD > 1. Total error on the $^{87}Sr/^{86}Sr$ used in calculation is 0.02%. The errors on the run from Cameca MS were $3–8 \cdot 10^{-5}$ and $1–2 \cdot 10^{-5}$ from Finnigan Mat.

Tab. 1 Isotope whole rock compositions in the Aar granite and the Grimsel granodiorite. In the Grimsel granodiorite, two different shear zones have been analyzed: ACII (3 meters width) and A or AD (80 meters width). The granite shear zone has a width of 4 meters (weight of samples: 4–8 kg).

No Samples	Rb ppm	Sr ppm	$^{87}Rb/^{86}Sr$	$^{87}Sr/^{86}Sr$	Distance m
Granite shear zone: Aar granite					
Undeformed rocks					
Aar1	240	72.2	9.78	0.74643	
Aar2	231	55	12.20	0.75617	
Aar3	216	177	5.34	0.72798	
Aar6	244	90.2	7.85	0.73592	
Orthogneiss					
ACIIIa	209	79.5	7.61	0.73345	2.4
ACIIIb	303	114	7.71	0.73980	2.6
ACIIIc	258	69.3	10.80	0.73966	2.8
ACIIIn	232	86.1	7.83	0.73381	2.0
ACIIIp	227	114	5.77	0.73232	0.0
Mylonites					
ACIIId	254	69.4	10.62	0.73936	3.0
ACIIIg	263	78.3	9.76	0.73722	3.4
ACIIIh	356	70.6	14.60	0.74380	3.8
ACIIIi	220	53.2	12.00	0.74518	4.0
Granodiorite shear zones: Grimsel granodiorite					
Undeformed rocks					
ACIGD	168	277	1.75	0.71309	
ACIIa	125	343	1.06	0.70937	0.0
AD13	115	399	0.84	0.70895	**0.0**
Orthogneiss					
A15	170	341	1.44	0.71151	
AD11	191	344	1.60	0.71177	
AD12	180	325	1.60	0.71124	
AD22	166	350	1.37	0.71085	
AD21	182	304	1.72	0.71445	
AD20	144	234	1.80	0.71039	
ACIIb	115	348			0.9
ACIIc	109	341			1.2
ACIId	140	333			1.5
ACIIcd	106	359	0.86	0.70920	1.7
ACIIfg	111	321	1.00	0.71123	2.8
ACIIh	148	188	2.28	0.71095	3.0
Mylonites					
A20	212	138	4.40	0.71419	**76.8**
AD23a	241	71.8	8.97	0.72203	**80.0**

Tab. 2 Isotope whole rock compositions in the Wassen granite. KAW analysis are taken from SCHALTEGGER (1990b). Samples GWC1, GWC2 and GWC3 have respectively been taken in three different shear zones of 10 m, 3 m and 1 m width. Samples GWC 3 f, g and h are granite mylonites at the contact with paragneisses. The bulk composition of these mylonites reflects initial magmatic variations for these border facies. These rocks are not used in shear zone studies (weight of samples: 4–8 kg).

No Samples	Rb ppm	Sr ppm	$^{87}Rb/^{86}Sr$	$^{87}Sr/^{86}Sr$	Distance m
Undeformed rocks: Wassen granite (SCHALTEGGER, 1989)					
KAW 899	156	208	2.17	0.71481	
KAW 900	145	210	1.99	0.71339	
KAW 2508	188	178	3.06	0.71876	
KAW 2511	167	65	7.44	0.73639	
KAW 2512	130	267	1.41	0.71156	
KAW 2513	150	176	2.47	0.71637	
KAW 2514	167	134	3.60	0.71884	
KAW 2517	175	144	3.52	0.72039	
KAW 2518	138	221	1.81	0.71238	
KAW 2519	135	246	1.59	0.71152	
KAW 2521	193	73	7.69	0.73578	
KAW 2522	148	145	2.96	0.71713	
KAW 2523	135	114	3.43	0.71950	
KAW 2541	151	178	2.45	0.71503	
Granite shear zones: Wassen granite					
Undeformed rocks					
GWC1a	164	150	3.17	0.71840	0.0
GWC1b	163	163	2.90	0.71798	1.3
GWC2a	135	149	2.68	0.71705	
GWC2b	171	142	3.49	0.71898	
Orthogneiss					
GWC1d	169	149	3.29	0.71885	2.8
GWC1f	187	111	4.88	0.71989	6.8
GWC1h	163	163	2.90	0.71647	9.5
GWC1i	186	132	4.08	0.71725	9.9
GWC2c	175	152	3.34	0.71851	
GWC2d	199	151	3.82	0.71833	
GWC3a	154	102	4.37	0.71720	**0.4**
GWC3b	131	108	3.51	0.71832	**0.0**
GWC3c	143	97	4.27	0.71916	**0.8**
GWC3d	148	111	3.86	0.71876	**0.9**
Mylonites					
GWC1j	205	125	4.75	0.71803	10.0
GWC2e	138	207	1.93	0.71756	
GWC3e	168	75	6.49	0.72046	**1.0**
GWC3f	150	102	4.26	0.72332	
GWC3g	147	64	6.66	0.72707	
GWC3h	144	84	4.97	0.72641	

Tab. 3 Isotope whole rock compositions in the Truzzo granite. G.73.XXX analyses are from GULSON (1973). Rocks named TC1, TC4 and TC5 have been sampled in three different shear zones of 3, 6 and 10 meters width respectively (weight of samples: 4–8 kg).

No Samples	Rb ppm	Sr ppm	$^{87}Rb/^{86}Sr$	$^{87}Sr/^{86}Sr$	Distance m
Undeformed rocks: Truzzo granite (GULSON, 1973)					
G.73.791	255	131	5.46	0.73650	
G.73.105/4	305	89.5	9.72	0.75200	
G.73.105/7	315	91.1	9.86	0.75340	
G.73.789	207	51.8	11.51	0.76270	
G.73.789/1	208	51.2	11.59	0.75970	
G.73.790	266	56.6	13.98	0.77060	
G.73.790/1	266	56.4	14.19	0.77070	
Granite shear zones: Truzzo granite					
Undeformed rocks					
TC1a	152	60.2	7.32	0.74256	
TC4a	226	99.8	6.57	0.73775	0.0
TC5a	192	139	4.02	0.72940	**0.0**
TC6a	254	114	6.46	0.73625	
HTC2	196	143	3.97	0.73070	
HTC4	185	135	3.90	0.72928	
Orthogneiss					
TC1f	139	70.8	5.70	0.73555	
TC4e	199	111	5.18	0.73080	5.4
TC4i	187	120	4.74	0.73007	5.7
TC5g	152	129	3.40	0.72543	**9.0**
TC5h	152	141	3.12	0.72545	**9.6**
Mylonites					
TC1g	104	84.7	3.57	0.73218	
TC1h	124	79.9	4.49	0.73348	
TC4g	181	128	4.09	0.72966	6.0
TC4h	186	125	4.31	0.73026	5.9
TC5i	135	164	2.38	0.72373	**9.8**
TC5j	109	237	1.33	0.72029	**10.0**